ISBN: 978-3-95450-248-6 ISSN: 2673-5490 doi: 10.18429/JACoW-IPAC2025-WECN2

FIRST BEAM COMMISSIONING OF THE HZB SRF PHOTOELECTRON GUN

T. Kamps[1]*,B. Alberdi, T. Birke, E. J. Brookes[1], J. Dube[1], P. Echevarria, D. Eichel, E. Ergenlik, R. Fleischhauer, A. Frahm, F. Hoffmann, H. Huck, A. Jankowiak[1], G. Klemz, J. Knobloch[2], J. Kolbe, J. Kühn, S. Lederer, S. Mistry, A. Neumann, N. Ohm, F. Pfloksch, H. Plötz, G. Rehm, S. Rotterdam, O. Schappeit, H. Stein, A. Ushakov, J. Ullrich, J. Völker, C. Wang[2], Helmholtz-Zentrum Berlin, Berlin, Germany
[1]also at Humboldt-Universität zu Berlin, Germany,
[2]also at Universität Siegen, Germany
A. Galdi, Università degli Studi di Salerno, Italy
I. Will, Max-Born Institut, Germany

Abstract

The versatile 1.3 GHz superconducting radio-frequency (SRF) gun at HZB successfully generated first photoemission beam from a high quantum efficiency (QE), multi-alkali photocathode. This demonstrates worldwide first beam operation of a SRF gun at high repetition rate and with a robust multi-alkali Na-based photoemission source. The setup of the test and all sub-systems is described. The latest results of SRF commissioning, photocathode QE measurements, and first beam parameter measurements are presented in the paper.

INTRODUCTION

The SRF photoinjector at SEALAB [1, 2] was designed in the framework of the bERLinPro project [3, 4]. Based on beam dynamics studies, a split photoinjector configuration was chosen, featuring separate SRF gun and SRF booster modules. The SRF gun was designed to generate a low emittance (normalized emittance of 1 µmrad at 77 pC bunch charge) electron beam with high average current, and to accelerate the beam to 2.5 MeV for subsequent acceleration and longitudinal beam profiling in the SRF booster. The installation and commissioning of the complete photoinjector was planned in stages. The first is the SRF photoelectron gun (SRF gun); in the second stage, the SRF booster will be installed.

In 2018, After a technical failure of the photocathode handling system inside the SRF gun during initial beam commissioning with a Cu and Cs-K-Sb photocathode [5], commissioning efforts were delayed due to the Corona pandemic (2020 to 2022) and a cyberattack on HZB in 2023. In summer 2024, we completed all technical work on the SRF gun, its photocathode handling system and the electron diagnostics beamline. This enabled the start of pre-beam checkout and the first cold SRF commissioning in autumn/winter 2024. We faced another technical issue related to a warm part of the high-power RF input windows. After the repair of the warm windows during winter 2024/2025, we commenced SRF commissioning in February 2025 culminating in the first beam in March 2025. The results presented here were all achieved during the first run with the beam, with 13 weeks of operation from March to May 2025. The goal for the first weeks was to achieve first beam generation, and begin to commission the SRF gun at low bunch charge (7 pC) and low average current (1 to 10 µA range) towards a linear beam optics operation mode with high wanted-to-unwanted beam ratio. In future operation, we aim to raise first the bunch charge to the design value of 77 pC, reach the design optics, and subsequently increase the average current into the 1 to 10 mA range.

* kamps@helmholtz-berlin.de

SETUP OF THE SRF GUN

Figure 1 describes the technical layout of the SRF gun, including the photocathode transfer dock and the first meter diagnostics section. The initial beam measurements were all performed using the viewscreen (FOM), beam position monitor (BPM), and Faraday cup (FCUP) diagnostics [6]. The beam current extracted from the photocathode can be measured with a cathode bias power supply. We installed a cathode camera to observe the cathode inside the SRF cavity back wall. The drive laser beam is guided through a vacuum window outside the SRF gun module and can be steered to the photocathode emission area.

SRF COMMISSIONING

Before attempting laser-on-cathode operation to produce first beam, the SRF cavity was commissioned to reach an operation point at which no unwanted beam generated by field emission was detected.

Figure 2 shows the performance development of the SRF gun cavity in the past years after selected treatment steps. We could reach in March 2025 gradients (peak on axis field) of 10 MV/m before dark current generation by field emission kicks in, then up to 26 MV/m with increasing dark current generation and eventual quench. For the initial commissioning phase, the cavity was run between 10 and 14 MV/m. After reaching the linear optics goal we want to process the cavity further towards 20 MV/m. With a digital LLRF system the phase stability varies between 0.07 and 05 deg

ISBN: 978-3-95450-248-6 ISSN: 2673-5490 doi: 10.18429/JACoW-IPAC2025-WECN2

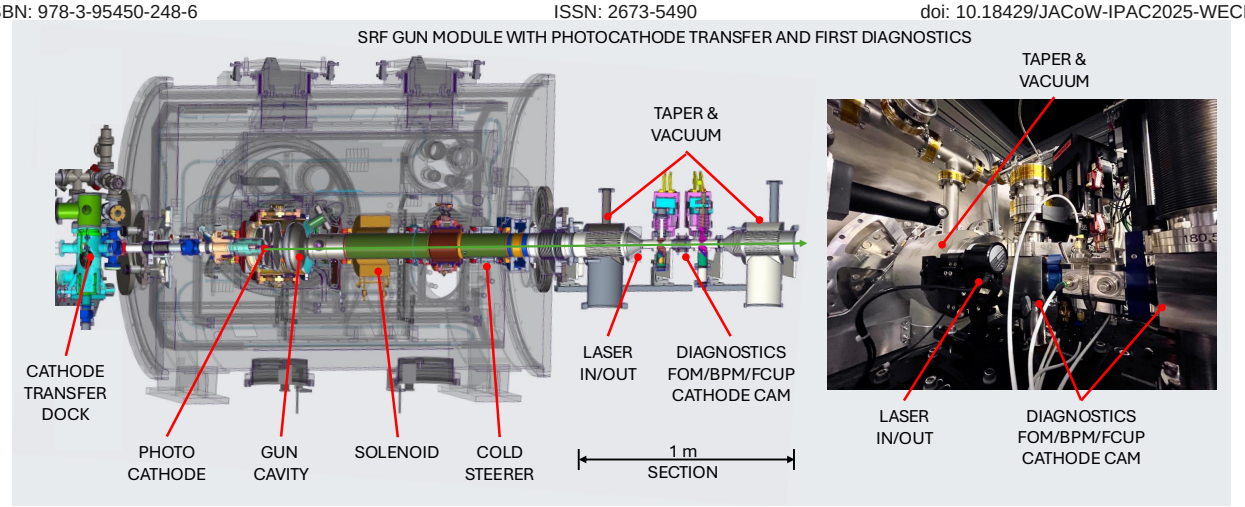

Figure 1: Left:Technical layout of the SRF gun system under investigation. Right: Photo of the first meter diagnostics section.

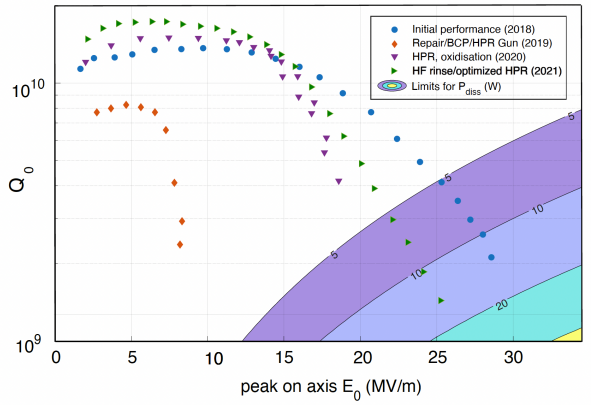

Figure 2: Evolution of intrinsic quality factor Q_0 vs. peak on axis field of the second gun cavity after production (in 2019) and through the refurbishments steps (2020 to 2021) following a damaging by the manufacturer [7]. Performance before operation is after HF rinsing and optimized HPR.

RMS, limited by instabilities in the cryogenic supplies. The amplitude stability is 1×10^{-3} dA/A.

DRIVE LASER PERFORMANCE

The drive laser was specified to produce variable, several-ps-long pulses at a 522 nm wavelength and 2 W in CW operation mode with a tunable repetition rate of up to 50 MHz. During the first 13 weeks of operation, the laser was typically operated at a 1 MHz repetition rate with a 4 ps (FWHM) pulse length. The drive laser is located in another part of the accelerator building with the beam transported to the accelerator tunnel through a 30 m long optical beamline. The transport efficiency is measured as 85 %. Nearby cooling water pumps introduced vibrations into the optical beamline which lead to challenges in the pointing stability. This problem was mitigated by using a relay imaging system for optical transport and inserting a variable beam-shaping aperture close to the cathode. The beam is expanded in front of the aperture such that pointing variations are subsequently blanked out with a reduction of laser power between 1 % and 10 % efficiency, depending on the chosen spot size. Pointing stability on the cathode is now below the measurement threshold, corresponding to less than 100 µm on the cathode. Most data in the initial 13 weeks was taken with a truncated Gaussian (close to flattop) laser spot of 2 mm diameter on the cathode. The laser operates with high power stability, slow long-term drift of less than 2 % and between 0.6 % to 1.5 % short-term fluctuations. Upcoming steps include stabilizing the long- and short-term drifts with a feedback system, improving the laser beam shaping system's efficiency, and pushing the repetition rate up to the design value of 50 MHz.

PHOTOEMISSION SOURCE

For commissioning of the SRF gun, a high-quantum-efficiency bialkali-antimonide Na-K-Sb photocathode was prepared and transported. This photocathode displayed a quantum efficiency of 2.5 % at 522 nm following preparation. The ternary system was chosen for its high electron yield and low intrinsic emittance, and can be illuminated with visible (green) light. The photocathodes are prepared on-site at the photocathode laboratory of HZB by simultaneous deposition of all three materials [8]. Following preparation, the photocathode was transferred to an UHV vacuum suitcase and moved to the UHV transfer system at the photoinjector [9]. The QE degraded by one order of magnitude during the transfer and lost another order of magnitude moving the cathode inside the transfer system from the warm section to the cold section of the SRF gun. To mitigate this effect in future operation, changes in the transfer chain of orientation of pumps and valves will be implemented, minimizing the risk of pressure bursts. In Fig. 3 the QE development of the photocathode during 13 weeks of operation is shown. The QE has been measured via the drain current of the photocathode bias voltage power supply with 5 kV bias and a laser power of about 1 mW. Several vacuum events produced pressure bursts in the 1×10^{-8} mbar range for more than one hour in front of the photoinjector, followed by a reduction of the QE. However, the QE recovered within a few days during RF operation. RF and beam operation even demonstrated

ISBN: 978-3-95450-248-6 ISSN: 2673-5490 doi: 10.18429/JACoW-IPAC2025-WECN2

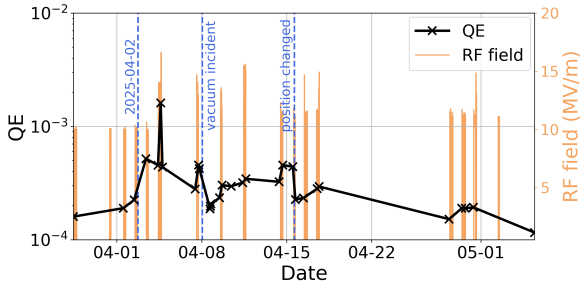

Figure 3: QE development in the gun measured with 1 mm laser spot size.

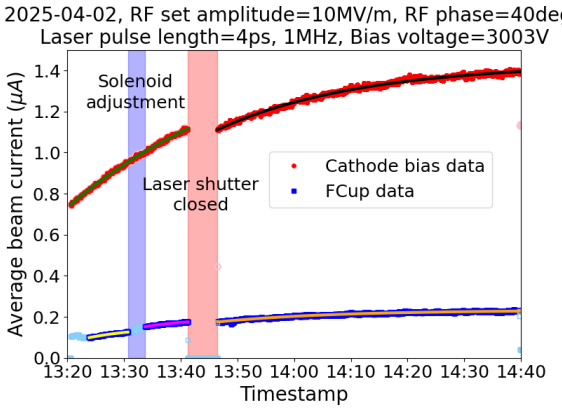

Figure 4: Beam current development over 1h20min of beam operation.

a positive impact on the QE. Field levels 16 MV/m can be correlated with an increase of the QE factor larger than a factor of six.

Figure 4 shows the increase of the beam current over several hours of operation with a constant RF field of a gradient of 10 MV/m, at constant laser power. The beam current was monitored from both the Faraday cup in the diagnostics section and from the drain current measured the cathode bias power supply, each showing an increase of the beam current over the measurement period. When extrapolated to 8 h of operation, the cathode bias data and the Faraday cup data indicate an increase in current from 0.7 µA to 1.6 µA, and 0.15 µA to 0.26 µA respectively. This indicates an increase by a roughly a factor of two in both cases. The time constant of the observed increase was consistent for both measurement styles of (25 ± 2) min. The lower current measured in the Faraday cup is attributed to losses originating from phase slippage and subsequent defocusing of electrons at the gradient of 10 MV/m. A significant fraction is thus not transported to the Faraday cup but is trapped inside the SRF cavity, causing losses on the cavity walls or reflected on axis towards the cathode surface. The transmission efficiency from the cathode to the Faraday cup improves with higher gradients, leading to shorter time constants, and higher current increases. The average short-term fluctuations in beam current are consistent with the measured variations in laser power fluctuations. QE maps taken regularly during operation revealed that the whole coated cathode film is rejuvenated, not just the area where the laser hits the cathode. The observed increase in QE and beam current suggests a rejuvenation mechanism of the cathode surface, possible hypotheses for which include electron back bombardment or RF field processing of the cathode film.

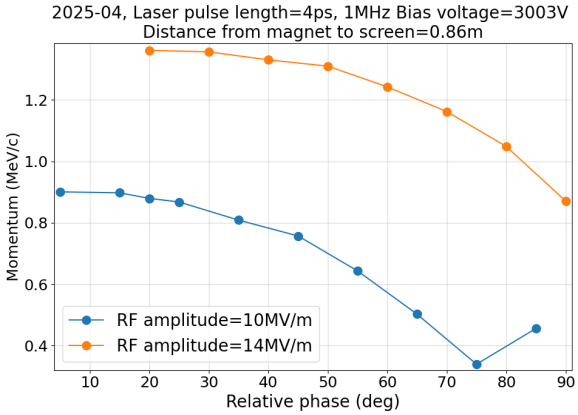

Figure 5: Momentum versus launch phase for two gradients.

BEAM MEASUREMENTS

After achieving first beam, the initial objective was to determine the optimal launch phase between laser and RF field to maximize energy gain. For the gradients before field emission kicks in, the energy versus phase curves proved to be relatively flat as can be seen in Fig. 5. This indicates a large energy spread, which contributes to beam loss. We also performed beam based alignment of the laser beam on the cathode to find the launch position that minimizes transverse deflection by the RF field. The next steps include beam based alignment in the solenoid, followed by emittance measurements.

CONCLUSIONS AND NEXT STEPS

We achieved first beam operation from a Na-K-Sb photcathode with high quantum efficiency in a SRF gun. First measurements at low accelerating gradients indicate that the Na-K-Sb is a promising electron source for SRF-based injector applications. No issues with multipacting were observed at low bias voltage, and the photocathode demonstrated stable, moderate QE levels over the course of a month. The observed increase in QE - by almost one order of magnitude - and the suggested QE/RF-processing mechanism justifies further investigation at higher accelerating gradients and starting at a higher QE level. Emittance measurements of the intrinsic cathode emittance and the beam dynamics contributions also require further studies. The SRF gun at SEALAB will support a wide range of possible experiments for accelerator research and development, covering a large range of beam parameter space from short pulse-low charge ultrafast scattering [10], up to full high brightness, high current ERL for HEP studies [11].

ISBN: 978-3-95450-248-6 ISSN: 2673-5490 doi: 10.18429/JACoW-IPAC2025-WECN2

REFERENCES

[1] T. Kamps *et al.*, "Accelerator Physics Experiments at the Versatile SRF Photoinjectior of SEALAB", in *Proc. IPAC'23*, Venice, Italy, 2023, pp. 2115–2118. doi:10.18429/JACoW-IPAC2023-TUPL160

[2] A. Neumann *et al.*, "bERLinPro Becomes SEALab: Status and Perspective of the Energy Recovery Linac at HZB", in *Proc. IPAC'22*, Bangkok, Thailand, Jun. 2022, pp. 1110–1113. doi:10.18429/JACoW-IPAC2022-TUPOPT048

[3] A. Jankowiak, J. Knobloch, N. Paulick, and B. Kuske, "Conceptual Design Report BERLinPro", 2012,

[4] M. Abo-Bakr *et al.*, "The Berlin Energy Recovery Linac Project BERLinPro - Status, Plans and Future Opportunities", in *Proc. ERL'19*, Berlin, Germany, Sep. 2019, pp. 8–13. doi:10.18429/JACoW-ERL2019-MOCOXBS04

[5] A. Neumann *et al.*, "The BERLinPro SRF Photoinjector System - From First RF Commissioning to First Beam", in *Proc. IPAC'18*, Vancouver, Canada, Apr.–May 2018, pp. 1660–1663. doi:10.18429/JACoW-IPAC2018-TUPML053

[6] E. Ergenlik *et al.*, "Instrumentation and operation modes for the commissioning phase of the SEALab SRF photoinjector", in *Proc. IPAC'23*, Venice, Italy, 2023, pp. 4703–4705. doi:10.18429/JACoW-IPAC2023-THPL103

[7] Ye. Tamashevich *et al.*, "Damage recovery for srf photoinjector cavities", *Engineering Research Express*, vol. 6, no. 2, p. 025009, May 2024. doi:10.1088/2631-8695/ad408a

[8] J. Dube *et al.*, "Triple evaporation of bialkali antimonide photocathodes and photoemission characterization at the photex experiment", 2025, arXiv: 2503.03573 [physics.acc-ph], https://arxiv.org/abs/2503.03573,

[9] J. Kühn *et al.*, "UHV Photocathode Plug Transfer Chain for the bERLinPro SRF-Photoinjector", in *Proc. IPAC'2017*, 2017. doi:JACoW-IPAC2017-TUPAB029

[10] B. Alberdi Esuain *et al.*, "Novel approach to push the limit of temporal resolution in ultrafast electron diffraction accelerators", *Sci. Rep.*, vol. 12, p. 13365, 2022. doi:10.1038/s41598-022-17453-z

[11] C. Adolphsen *et al.*, *European Strategy for Particle Physics – Accelerator R&D Roadmap*. CERN, Mar. 2022. doi:10.23731/CYRM-2022-001